# Supplementary Tables and Figures

## Ferrimagnetic structures with rare-earth induced spin-reorientation in the Mn self-doped perovskite $(Er_{0.7}Mn_{0.3})MnO_3$

Andreas Dönni, Vladimir Y. Pomjakushin, Martin Rotter, Lei Zhang, Kazunari Yamaura, Alexei A. Belik

**Supplementary Table S1.** Energy levels of the crystal field (CF) splitting of $Er^{3+}$ in $(Er_{0.7}Mn_{0.3})MnO_3$ and $(Er_{0.8}Mn_{0.2})MnO_3$ based on the point charge model, calculated by McPhase.

| Number of CF level | $(Er_{0.7}Mn_{0.3})MnO_3$ $Er^{3+}$ energy (meV) | | $(Er_{0.8}Mn_{0.2})MnO_3$ $Er^{3+}$ energy (meV) | |
|---|---|---|---|---|
| 16 | 23.72 | 36.96(39) | 23.25 | 36.36(39) |
| 15 | 23.72 | 36.96(39) | 23.25 | 36.36(39) |
| 14 | 12.63 | 25.87(25) | 12.36 | 25.48(23) |
| 13 | 12.63 | 25.87(25) | 12.36 | 25.48(23) |
| 12 | 4.12 | 17.36(20) | 3.63 | 16.75(16) |
| 11 | 4.12 | 17.36(20) | 3.63 | 16.75(16) |
| 10 | -0.70 | 12.54(25) | -0.99 | 12.13(27) |
| 9 | -0.70 | 12.54(25) | -0.99 | 12.13(27) |
| 8 | -6.54 | 6.70(16) | -6.13 | 6.99(17) |
| 7 | -6.54 | 6.70(16) | -6.13 | 6.99(17) |
| 6 | -9.69 | 3.55(25) | -8.76 | 4.36(32) |
| 5 | -9.69 | 3.55(25) | -8.76 | 4.36(32) |
| 4 | -10.32 | 2.92(27) | -10.24 | 2.88(13) |
| 3 | -10.32 | 2.92(27) | -10.24 | 2.88(13) |
| 2 | -13.24 | 0.00(0) | -13.12 | 0.00(0) |
| 1 | -13.24 | 0.00 | -13.12 | 0.00 |

**Supplementary Table S2.** Induced magnetic $Er^{3+}$ moments in $(Er_{0.8}Mn_{0.2})MnO_3$ at $T = 1$ K in an external magnetic field of $H = 10$ T applied along the three axes $a$, $b$, $c$ calculated by McPhase. Uncertainties due to the experimental errors in the crystal-structural parameters were evaluated using gauss law of error propagation and are shown in parentheses only for $Er1_1$ for simplicity.

| $H \parallel a$ | $\langle M_a \rangle$ | $\langle M_b \rangle$ | $\langle M_c \rangle$ | $\langle M \rangle$ |
|---|---|---|---|---|
| $Er1_1$ | 3.112(755) | 0(0) | -1.795(210) | 3.592(763) |
| $Er1_2$ | 3.112 | 0 | 1.795 | 3.592 |
| $Er1_3$ | 3.112 | 0 | -1.795 | 3.592 |
| $Er1_4$ | 3.112 | 0 | 1.795 | 3.592 |
| $H \parallel b$ | $\langle M_a \rangle$ | $\langle M_b \rangle$ | $\langle M_c \rangle$ | $\langle M \rangle$ |
| $Er1_1$ | 0(0) | 8.269(33) | 0(0) | 8.269(33) |
| $Er1_2$ | 0 | 8.269 | 0 | 8.269 |
| $Er1_3$ | 0 | 8.269 | 0 | 8.269 |
| $Er1_4$ | 0 | 8.269 | 0 | 8.269 |
| $H \parallel c$ | $\langle M_a \rangle$ | $\langle M_b \rangle$ | $\langle M_c \rangle$ | $\langle M \rangle$ |
| $Er1_1$ | -0.838(43) | 0(0) | 5.765(168) | 5.826(172) |
| $Er1_2$ | 0.838 | 0 | 5.765 | 5.826 |
| $Er1_3$ | -0.838 | 0 | 5.765 | 5.826 |
| $Er1_4$ | 0.838 | 0 | 5.765 | 5.826 |

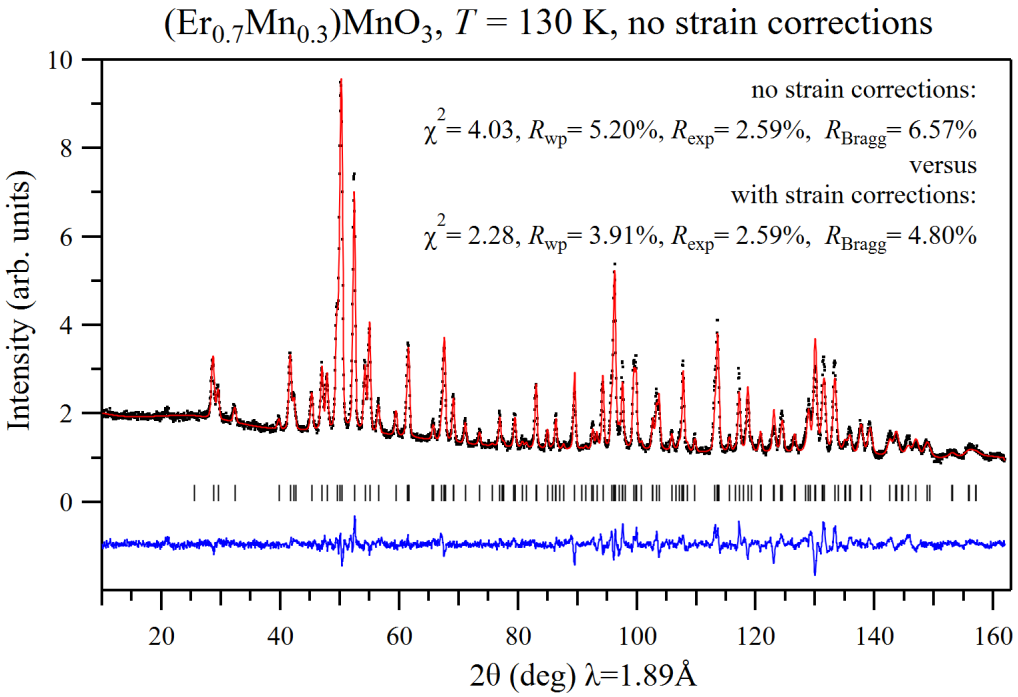


**Supplementary Fig. S1.** Experimental (black dots), calculated (red line), and difference (blue line) neutron diffraction pattern of $(Er_{0.7}Mn_{0.3})MnO_3$ in the paramagnetic state at $T$ = 130 K. No corrections for strain effects were used. The tick marks indicate Bragg peak positions of the crystal structure. Resultant $R$ and $\chi^2$ values with and without strain corrections are given.

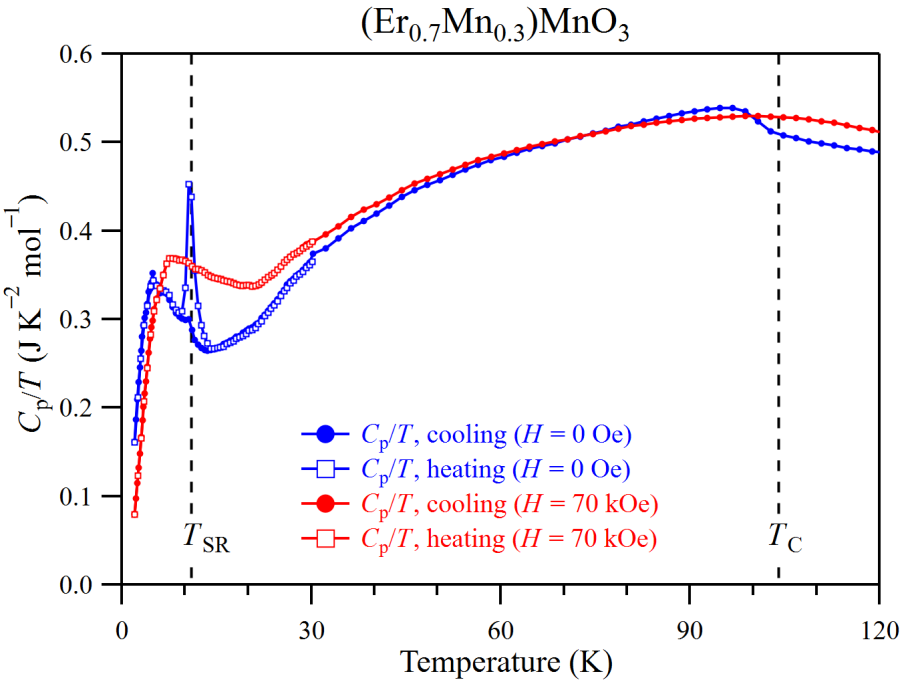


**Supplementary Fig. S2.** Temperature dependence of specific heat Cp/T of $(Er_{0.7}Mn_{0.3})MnO_3$ measured on cooling (filled symbols) and heating (empty symbols) at magnetic fields $H = 0$ Oe and $H = 70$ kOe. The vertical dashed lines indicate the FiM phase transition at $T_C = 104$ K and the Spin-reorientation temperature at $T_{SR} = 11$ K at zero field.

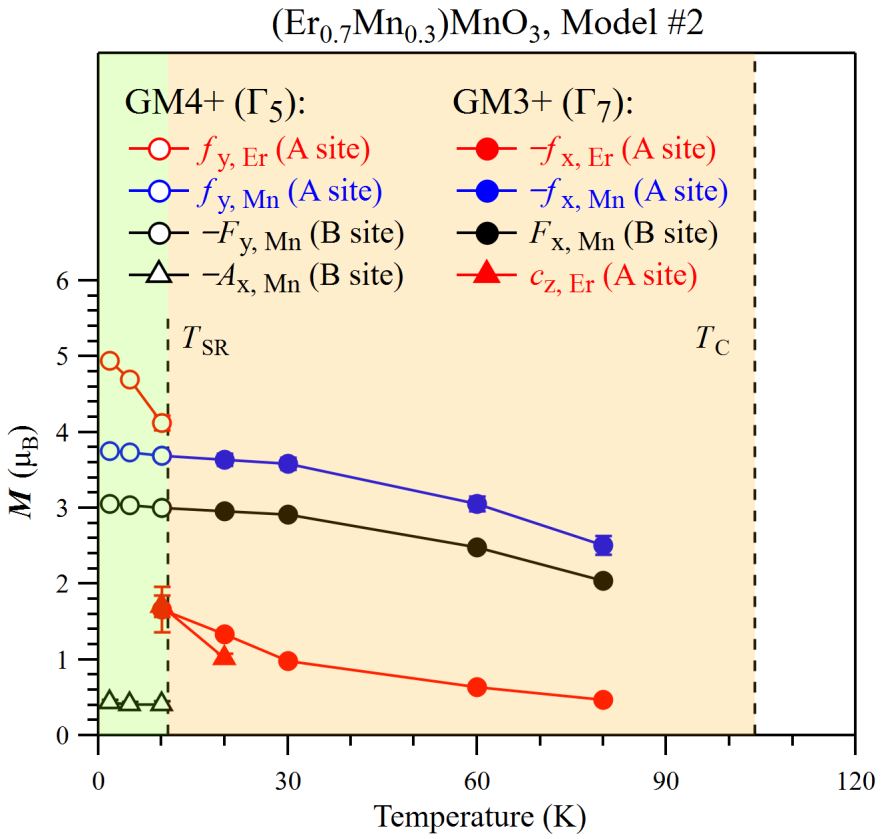


**Supplementary Fig. S3.** Temperature dependence of the ordered Mn and Er moments of $(Er_{0.7}Mn_{0.3})MnO_3$ based on Model #2. The vertical dashed lines indicate the FiM phase transition at $T_C$ = 104 K and the Spin-reorientation temperature at $T_{SR}$ = 11 K.

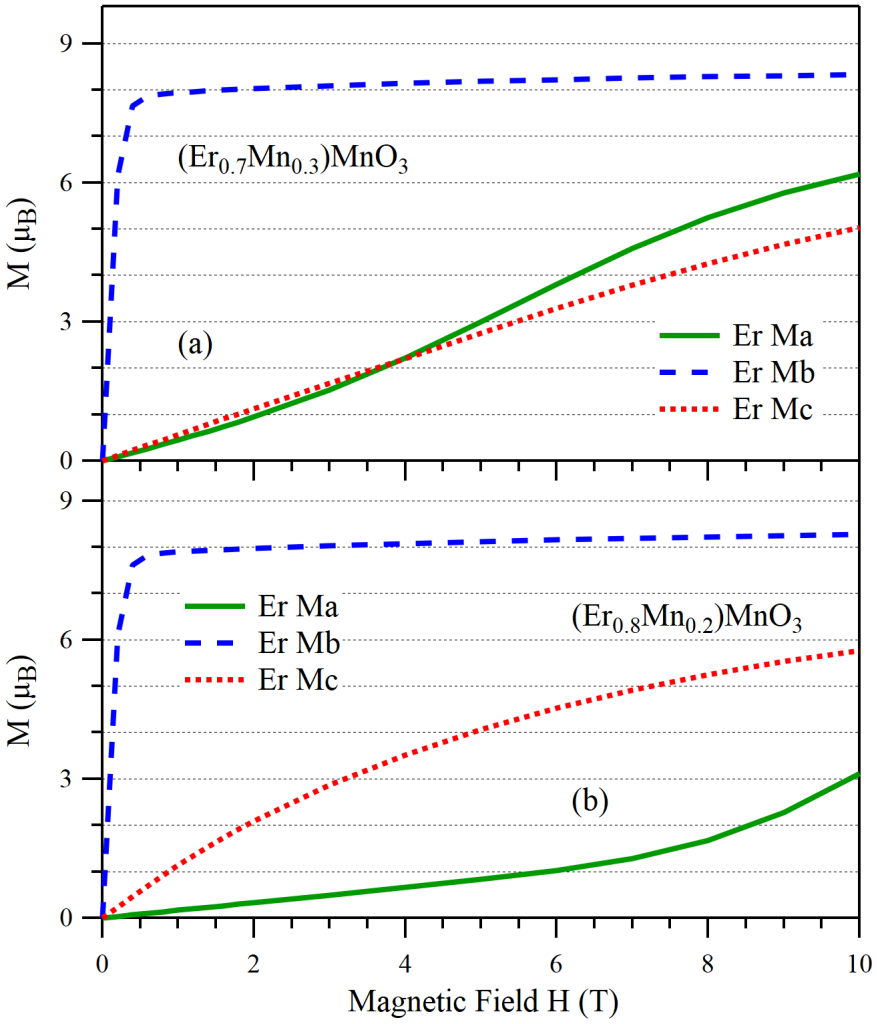


**Supplementary Fig. S4.** Field dependence of the single-ion magnetization in an external magnetic field applied along the *a*-, *b*- and *c*-axes for $Er^{3+}$ in $(Er_{0.7}Mn_{0.3})MnO_3$ (a) and $(Er_{0.8}Mn_{0.2})MnO_3$ (b) at $T$= 1 K calculated by McPhase.